Multivariate analysis of data from fabrication, testing and operation of a large lead/acid peak-shaving battery

Sam P. Perone*, Robert Petesch and Pei-Hwei Chen
Department of Chemistry, San Jose State University, San Jose, CA 95192 (USA)

William C. Spindler
Batteries Included, 15174 Kellen Ct., Riverside, CA 92506 (USA)

Sanjay L. Deshpandé
GNB Industrial Battery Co., 829 Parkview Boulevard, Lombard, IL 60148 (USA)

(Received June 7; 1991; in revised form August 12, 1991)

Abstract

Statistical, pattern recognition and cluster analysis studies have been applied to the cumulative data base documenting the fabrication, testing and operating history since 1983 of a large lead/acid energy storage battery (500 kW h, 324 cells). Results show that fabrication and formation parameters have a significant influence on initial measured cell properties and, even more importantly, appear to have a continued impact on cell performance throughout battery life. Moreover, it appears that performances of individual mature cells can be predicted from multivariate analysis of initial fabrication/test data or of routine cell maintenance data. Correlations between cluster analysis observations and cell capacity trends, and early cell failure occurrences, underscore the value of multivariate analysis of fabrication data. The ultimate goal of cell lifetime prediction from initial fabrication/test data will be evaluated as large numbers of cell approach failure.

Introduction

The objective of this work has been to examine multivariate relationships among data obtained during fabrication, maintenance and capacity testing of lead/acid cells used in deep cycling energy storage applications, and to evaluate their correlation with cell performance and lifetime. This study began with the production of 340 large motive power (GNB, Inc., 2080 A h) lead/acid cells. Specifications were established by the Electric Power Research Institute. Fabrication materials and procedures were documented in detail and associated with individually numbered cells. Cells were produced and formed sequentially in batches of 80 cells, and a 5th batch of 20. These series-connected formation groups are referred to as circuits 1 to 5. Manufacturer data collection also included cell dry/wet weights, specific gravities, amounts of acid or water added, as well as capacity and voltage trends during five formation cycles.

Fifty-four 6-cell modules were installed at the Battery Energy Storage Test (BEST) Facility (operated by Public Service Electric and Gas Co. for EPRI), and acceptance tests were completed Dec. 7, 1983. The basic performance requirement was to

*Author to whom correspondence should be addressed.

0378-7753/92/$5.00

deliver 500 kW h, at 500 kW for 1 h. At this rate the cell capacity limit was set at 1040 A h. For a 5-h discharge at the 2080 A h cell capacity, 1.2 MW h of stored energy could be delivered. The battery was provided with an 8-year warranty. The modules at the BEST Facility were connected either in a single series string, or in three parallel strings of 18 modules each. The battery underwent over 200 intermittent test cycles for various utility and customer applications over a 4-year period. Data collected during that time included periodic maintenance measurements (specific gravities; water adjustments), and periodic capacity checks (cell capacities; float voltages; discharge voltage trends).

In July 1987, the battery was transported to and installed at Crescent Electric Membership Corporation (CEMC), Statesville, NC, an area electric power distributor. Since that time it has been operated in a peak-shaving environment, to discharge at a maximum power of 500 kW for 1 h, or a minimum power of 200 kW for 3 h. Periodic maintenance data, cell impedance measurements and cell failure observations have been added to the cumulative data base. In addition, capacity test data for a carefully selected subset of 109 to 121 of the 340 cells were obtained at CEMC in Mar. 1989 and Apr. 1990. Prior to Oct. 1990, only one cell had been bypassed, due to low capacity. In Oct. 1990, 44 cells, distributed among 11 modules, were observed to exhibit noticeable case swelling.

Statistical, pattern recognition and cluster analysis studies have been applied to the cumulative data base at each stage of the battery's life: after initial fabrication and testing; after cycle testing at BEST; and after more than three years of operation at CEMC. Results show that fabrication and formation parameters have a profound influence on initial and subsequently measured cell properties. Distinct cell subsets in circuits 1 and 3 appear related to known variations in materials, while circuits 2 and 4 include cell subsets related to physical placement during formation.

Cluster analysis studies of capacity test data from the BEST Facility showed that the same cell subsets identified from earlier examination of initial fabrication/formation data were also observed to exhibit common multivariate properties during this early-life operation. This suggests that early-life cell performance is impacted significantly, and predictably, by known materials/formation variations. Later studies of capacity data at CEMC confirmed that these same clusters of cells with common origins continue to exhibit similar performance behavior even into the battery's mid-life period.

Detailed descriptions of useful data descriptors, cumulative data analyses, observations, and conclusions are reported below.

Description of computer data base

All data are contained in a SYMPHONY™ data base management system, operated on an IBM/AT personal computer system. The entire data base currently includes over 50 000 raw data items, plus an equivalent number of computed data descriptors.

Data analysis methods

Basic statistical computations (averages, variances, distributions, maxima, minima, etc.) and associated graphical procedures were conducted using packages contained within SYMPHONY. Multivariate analysis procedures (correlation analysis, cluster analysis, pattern recognition and non-linear mapping) were developed for operation on the IBM/AT computer and programmed in compiled BASIC (Microsoft). Several general references exist for the multivariate analysis techniques used in these studies [1–4]. Specific references for the non-linear mapping [5, 6] and clustering [7] procedures are also available. A brief introduction to the pattern recognition techniques used in this work is provided here.

Pattern recognition involves the perception of regularities among sets of measurements describing objects or events. It is concerned with processing large amounts of data, the extraction of useful descriptors which concentrate the information content, and the development of criteria for examining those descriptors and recognizing the different classes to which each object belongs.

A pattern is defined as a d-dimensional vector composed of d independent measurements, and can be represented by:

$$P = w_1x_1 + w_2x_2 + w_3x_3 + \ldots + w_dx_d \tag{1}$$

where x_1, x_2, x_3, ... x_d are components (measurements) of the pattern vector; w_1, w_2, w_3, ... w_d are components of the weight vector; d is the number of dimensions.

Because the raw data vector may be of a large dimension, some reduction of dimensionality is desired to obtain reliable classification. Thus, a reduced set of N features is extracted from the data which may include combinations and transformations of the raw data (where $N<d$). This reduced feature set should be defined to best characterize the distinguishing properties of each class. Numerous systematic techniques have been applied to this task of feature selection, including correlation analysis, statistical distribution analysis, and empirical methods such as sequential iterative feature elimination.

Pattern classification was done in this work by applying the K-nearest neighbor classification rule. That is, the class of an unknown item is determined by the majority class of its K nearest neighbors in N-dimensional feature space. K is an odd number, usually one. The inter-item distances in feature space are calculated using Euclidian geometry, where:

$$D_{ij} = \left[\sum_{n=1}^{N} (X_{in} - X_{jn})^2 \right]^{1/2} \tag{2}$$

i, j = specific items, n = index for all features, N = total number of features.

Procedurally, the appropriate combination of features (and weights) which will provide high classification accuracy is found by examining a *training set* of patterns where each item has a known class. When this procedure is completed satisfactorily, a *prediction set* of known patterns can be examined where this set has the same origins as the training set, but has not been part of the training procedure. If high accuracy pattern classification is also obtained with the prediction set, the classification criteria can be considered valid and reliable. It would then be possible to apply these same criteria to true unknown items for classification, again provided the unknown items have the same origins and the same data structure as the original training set.

Results and discussion

Earlier work has been published describing multivariate analysis of battery test data and initial attempts at battery lifetime prediction from manufacturer's fabrication/test data [7, 8]. Earlier studies of the GNB battery system have also been reported [9–12]. The first of these latter reports [9] contained a summary of all factory data. The second report [10] examined manufacturer's data to identify inherent clusters of cells with common multivariate properties. The third and fourth reports [11, 12] examined performances of individual cells during operation of the battery system both at the BEST Facility and during the years at CEMC, and observed continued correlations with initial fabrication parameters. This report will examine the battery system as it enters the final phase of operations at CEMC; determine whether the same multivariate dependence on fabrication parameters continues to describe performance; evaluate the performance–predictive information content of routine maintenance data; and begin to examine statistically the occurrences of cell failures. In order to do this some review of past observations is required.

Manufacturer's fabrication/test data

Several useful descriptors (features) were extracted from the initial data base and used for statistical and multivariate data analysis. These descriptors are summarized in Table 1. Temperature data were also collected, but were used only for correcting specific gravities and capacities to standard conditions (77 °F).

Statistical analyses of initial fabrication/test data showed that significant differences existed for the mean values of 80% of the measured variables among the five formation circuits [10, 11].

When data from groups of cells from the same formation circuit were examined, using multivariate cluster analysis, several strong clusters were observed, depending on which groups of features were taken. Particularly strong clustering into two distinct subsets was observed for cells in circuit 1 and in circuit 3. Figure 1, for example, illustrates the distinct clustering observed in a seven-dimensional feature space. The figure is a non-linear mapping [5, 6] (two-dimensional) graphical representation of the clustering. From examination of the manufacturer's documentation, this observed clustering could be associated with whether grids or pasted plates were fabricated from 'old' or 'new' stock materials, which were distributed as indicated in Table 2. Observed clustering in circuits 1 and 3 closely matched the subsets defined in Table 2.

TABLE 1

Useful features (descriptors) from factory data base

Feature	Definition
ASHPA	Final acid adjustment before shipping
AVCAP	Average capacity over 5 test cycles
AVSA, AVSB	Average SGA, SGB, over 5 test cycles
CAPSLFA	Total acid in cell before 5th test cycle
DRYWT	Cell weight before acid addition
EQWC	Acid added (equalization) before 5th cycle
EQWF	Acid added in formation equalization step
FINLWT	Total weight of cell after formation equalization
INDL	AVCAP/RNGCAP
MNCAP, MXCAP	Minimum/maximum capacity of 5 test cycles
MNSA, MXSA	Minimum/maximum SGA over 5 test cycles
RELFRMA	EQWF/(FINLWT-DRYWT)
RNGCAP	(MXCAP-MNCAP)
RNGSA	(MXSA-MNSA)
SGA, SGB	Specific gravity after/before discharge each cycle
SG2	Specific gravity prior to formation equalization
SG4	Specific gravity prior to 5th cycle equalization
SHPSLFA	Total acid in cell as shipped

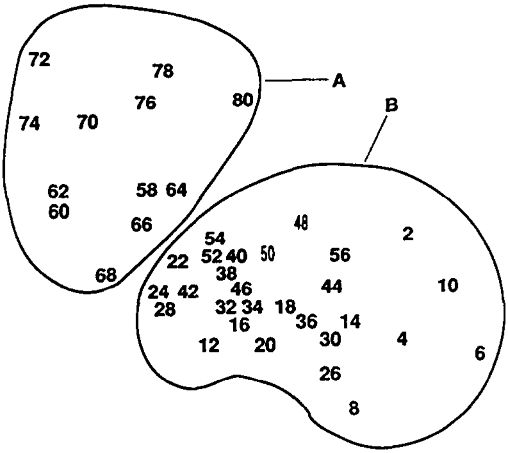

Fig. 1. Non-linear mapping (NLM) of seven-dimensional feature space for fabrication/test data, GNB cells, circuit 3 only. Mapping data for even-numbered cells (162–240), identified as 2–80. A = new/new grid/paste; B = old/new grid/paste. Features: DRYWT, EQWF, MXCAP, MNCAP, AVCAP, MXSA, RNSGA.

TABLE 2

Summary of materials changes for GNB cells

Subset	Circuit	Cells	Grid	Pasted plate
(a)	1	1–15	old	old
(b)	1	16–80	old	new
(c)	3	161–218	old	new
(d)	3	219–240	new	new

It should be pointed out that these observed variations within groups of cells fabricated and formed under presumably uniform conditions were not anticipated. The known variations in fabrication materials were not expected to contribute to any significantly different cell properties, as all batches of materials met procurement specifications for chemical and physical characteristics. Thus, their clear impact is a significant observation, perhaps warranting closer scrutiny in the future.

Examination of initial test data for cells from circuits 2 and 4 was of interest because there were no known changes in fabrication materials or procedures within these circuits. Cluster analysis, however, revealed distinct cell subsets with common multivariate properties. Figure 2 illustrates the clustering observed in a six-dimensional feature space. The cell groups selected for highlighting were those identified first by hierarchical clustering methods [7]. Examination of fabrication procedures showed that the different clustered subsets of cells could be associated with physical placement of those cells during formation cycles. Cells from interior locations (group A) of formation circuits tended to cluster together and separately from cells of outer locations (group B).

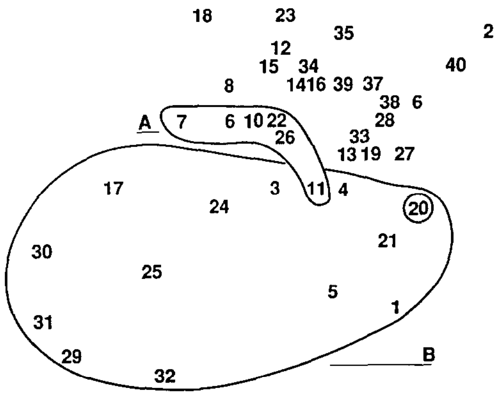

Fig. 2. Non-linear mapping (NLM) of six-dimensional feature space for fabrication/test data, GNB cells, circuit 2 only. Mapping data for cells 81–120, identified as 1–40. A = interior cells; B = exterior cells. Features: SG2, EQWF, MNCAP, AVCAP, AVSA, RNSGA.

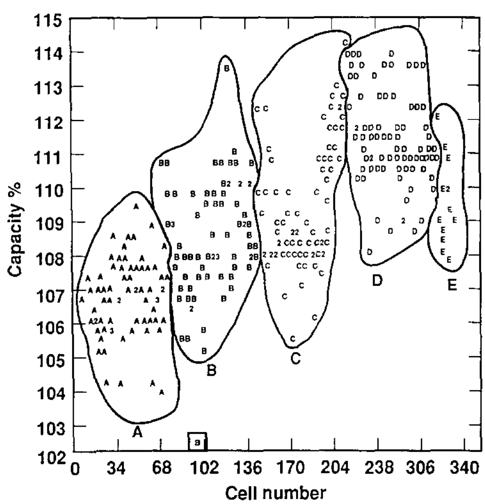

Fig. 3. Individual GNB cell capacities measured at BEST Facility, Jan. 1986. Groups A–E correspond to cells from original formation circuits 1–5. Discharge current, 346.6 A, 1.7 V cutoff. Capacities corrected to 25 °C. 324 total cells tested.

Data from BEST cycle testing

Battery maintenance data (electrolyte levels, water additions, specific gravities, cell float voltages and impedances) were obtained periodically during operation of the GNB 500 kW h battery at the BEST Facility from 1983–1987. In addition, a full capacity test was conducted in Jan. 1986, and data obtained included voltage–time, cumulative A h versus time, specific gravities before and after cycling, and float voltage levels. Capacity values were obtained with procedures identical to those used initially at GNB.

Figure 3 illustrates the underlying dependence of capacity on cell (and circuit) number. The increasing capacity can be associated with a learning curve in the manufacturing process, as circuit 1 represents the first batch of cells produced, whereas circuit 5 represents the last batch. There were documented [9] changes in fabrication procedures (most notably in the amount of acid added) between cells for circuits 1 and all following circuits. (For circuit 1 cells the initial acid fill provided a specific gravity of 1.230, whereas specific gravity for cells of circuit 2–5 was 1.260. All cells were adjusted to 1.285 before shipment.) In addition, the oldest materials on hand were used for cells in circuit 1 (Table 2).

Multivariate cluster analysis was applied to the BEST capacity test data, using features selected from the data descriptors defined in Table 3. All of the cluster sets revealed by analysis of factory data or BEST capacity data, along with the feature sets eliciting each cluster, are summarized in Table 4. Groups G1–G4 were observed initially from factory data. Groups G5–G7 were observed from BEST capacity test data. Groups G1, G3 and G4 were also observed with features selected from the BEST capacity data. Thus, clustering associated with changes in fabrication materials (groups G1 and G3) continued to be observed in the BEST data. (Figure 4 illustrates obvious clustering of cell capacities related to fabrication materials changes in circuit 3). Clustering related to variations in physical placement during formation (groups G2 and G4) was less pronounced for the BEST data, suggesting that perhaps this factor became less important during early cell life. The significance of the new clusters (G5–G7) observed from analysis of the BEST capacity test data is not yet understood. There are no known material variations associated with these clusters. Possible common environmental effects may be a factor (e.g. for group G7, the two cells are positioned adjacently at the negative terminal of one of three 108-cell strings).

Data from CEMC operations

Battery maintenance data were collected at CEMC as described for the operation at the BEST Facility. In addition, capacity tests were conducted in Mar. 1989 and Apr. 1990, with data collected in the same manner as for the 1986 test at the BEST Facility, except that only a selected group of 109–121 of the 324 operating cells was monitored. This subset was carefully selected to be representative of all cluster groups previously observed (Table 4), as well as to provide appropriate 'control' sets with

TABLE 3

Useful features (descriptors) from capacity test data

Feature	Definition
NCAP	Cell capacity during test cycle N
NFVLT	Float voltage after test cycle N
NV*xxx*	Cell voltage at *xxx* % nominal capacity
NSGB, NSGA	Specific gravity before/after discharge N
DLCPNN	Capacity change from one capacity test to the next
NDLV*x*. *y*	Cell voltage change beyond nominal capacity, where x, y = 8, 5, 0 for 108, 105, 100% capacity
	where N = F, from fabrication/test data B, from BEST capacity test cycle C, from CEMC capacity test cycle

TABLE 4

Cell clusters observed from factory and BEST data

Group	Subsets	Cluster analysis features
G1	O/O grid/paste	DRYWT, AVSA, EQWF, SG4
(Circuit 1)	O/N grid/paste	
G2	outer cells	SG2, EQWF, MNCAP,
(Circuit 2)	inner cells	AVCAP, AVSA, RNGSA
G3	O/N grid/paste	DRYWT, EQWF, MXCAP, MNCAP,
(Circuit 3)	N/N grid/paste	AVCAP, MXSA, RNGSA
G4	outer cells	SG2, EQWF, MNCAP, AVCAP,
(Circuit 4)	inner cells	AVSA, RNGSA
G5	6-cell cluster	BCAP, DLCPBF, BFVLT,
(Circuit 1)	(17, 21, 25, 36, 65, 74)	BV108, BDLV8.0
G6	9-cell cluster	BCAP, BV108, BDLV8.0
(Circuit 2)	(81, 82, 124, 128, 137, 139, 142, 143, 155)	
G7	2-cell cluster	BCAP, DLCPBF, BFVLT,
(Circuit 2)	(105, 109)	BV108, BDLV5.0

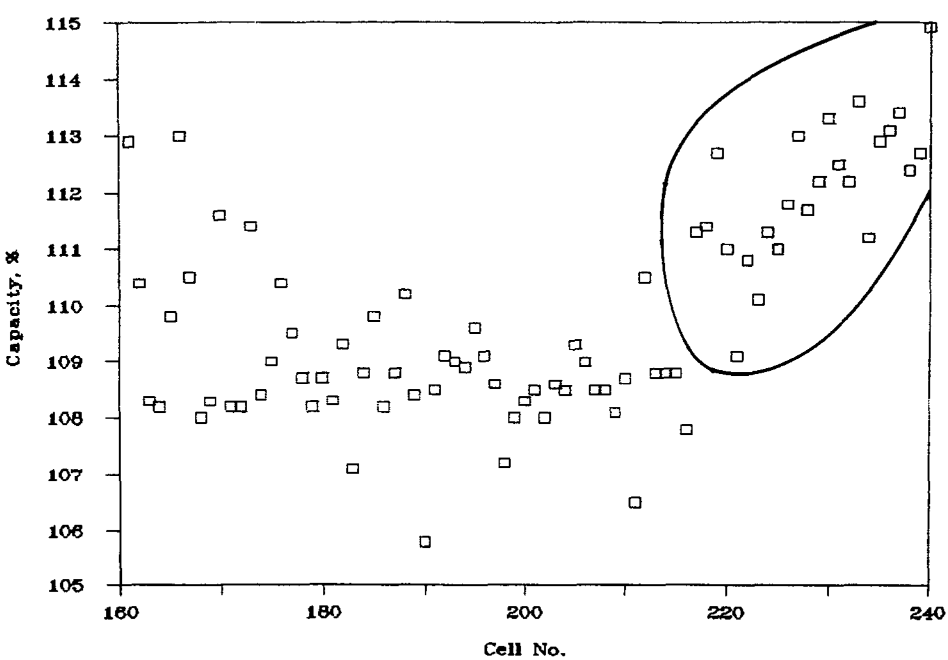

Fig. 4. Individual GNB cell capacities measured at BEST Facility, Jan. 1986, formation circuit 3 cells. 80 cells, 161–240. (See Table 2 for sub-sets.)

which each cluster group could be compared. Thus, statistically sound conclusions could be made regarding observed differences in behavior of previously identified cell clusters. Our discussion will focus on capacity data as the primary performance indicator.

Distributions

Capacity values appear normally distributed with a single maximum in each distribution for the 450 A discharges conducted in Mar. 1989 and Apr. 1990 (see Fig. 5(a) and (b)). The absence of any obviously unusual structure in the overall capacity distributions does not preclude the existence of sub-groups of cells with uniform but distinctive properties (see discussion below).

Statistical tests

Table 5 summarizes the results of examining performance, in the CEMC capacity tests, of the various cell subsets identified in earlier capacity tests (Table 4), and comparing them with 'control' sets. The purpose was to determine if groups of cells identified as having common *initial* properties, based on multivariate cluster analysis of data collected at the beginning of life, would continue to exhibit distinctly different performance characteristics at this stage of their lifetime (6–7 years).

Procedurally, each cell cluster of interest (identified as groups G1–G7 in Table 4) was compared either with another known cluster of cells taken from the same fabrication circuit, or with an appropriate 'control' subset, to determine if there was a *significant* difference in average capacity values between compared sets. (Control sets were composed of cells from the same fabrication circuit, which were known from previous cluster analysis studies to not be part of the cell cluster of interest, nor of any other observed clusters.) The statistical test used was Student's t-test, evaluated at the 95% confidence level [13].

The 1989 results in Table 5 examine the mid-life behavior of the GNB cells, and indicate that, in all but 2 cases, capacity values for the previously identified cluster groups were significantly different from control sets. Two exceptions are those clusters previously associated with inner/outer locations in formation corrals. Thus, it appears that the effects of material variations on performance continued to be observed; the performance variations related to environmental factors during early life (BEST data) also continued to be observed; and the effects of physical placement during formation became less important during mid-life operation.

The 1990 results in Table 5 examine cell behavior as the battery entered the end-of-life phase of operation. Statistical test results were virtually identical to those from 1989, except that for group G5 there was no longer a significant difference in capacities between the previously observed cluster and the control set. It is important to note, however, that the material-dependent clusters (groups G1 and G3) continue to show a significant difference in performance even as the cells approach end-of-life.

Pattern recognition performance prediction

One of the primary objectives of this study has been to determine if it is possible to predict individual cell performance from multivariate examination of initial fabrication/test data or periodic maintenance data. In the first case, the benefit would be that predicted better- or worse-performing cells could be identified at the outset and pre-selected for appropriate applications. More importantly, identification of those fabrication parameters affecting performance variance should have a positive impact on manufacturing practices.

From the results of cluster analysis studies described above, where capacity was the performance measure used, there appear to be sub-groups of cells within the same

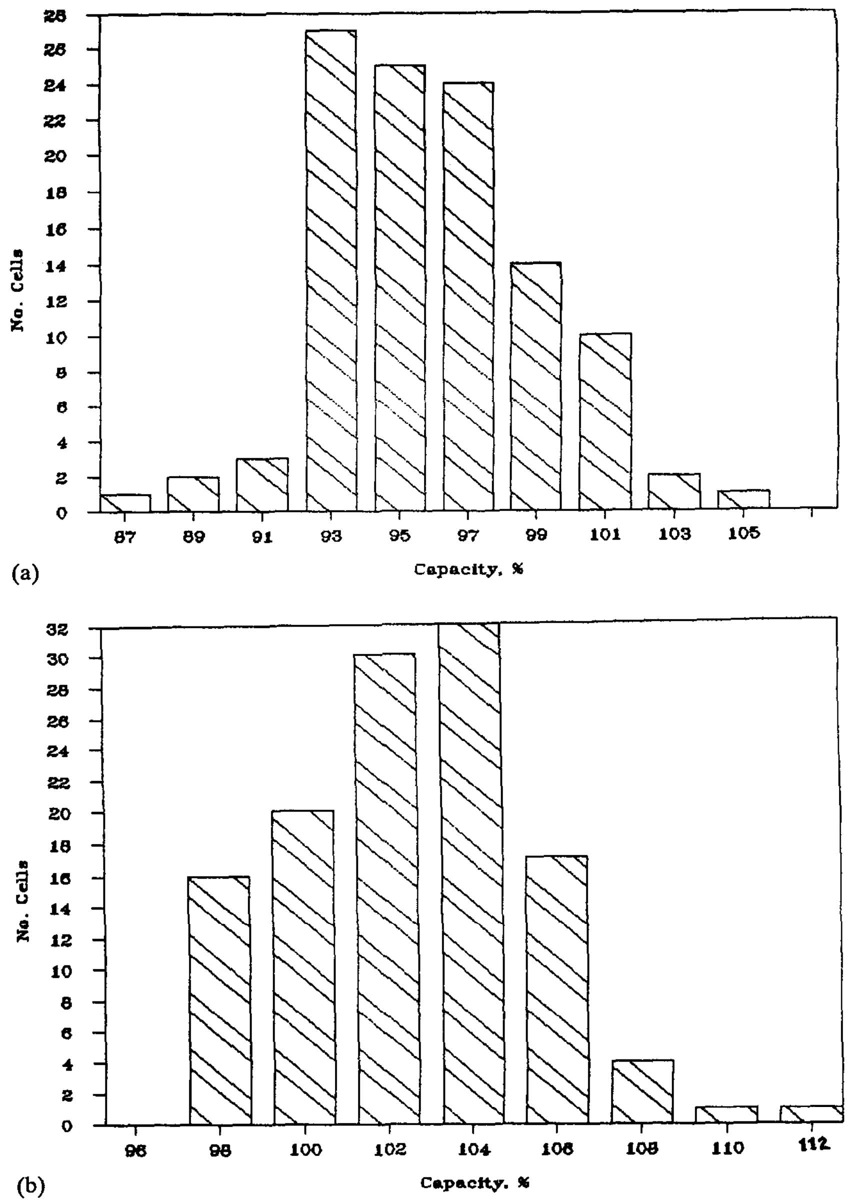

Fig. 5. Distributions of GNB cell capacities. Discharge currents, 450 A, 1.7 V cutoff; capacities corrected to 25 °C. (a) Capacity test at CEMC, Mar. 1989, 109 cells; (b) capacity test at CEMC, Apr. 1990, 121 cells, including all cells from (a).

batches (circuits) which have significantly different performance than other sub-groups. These sub-groups were identified by *unsupervised* multivariate cluster analysis; but these results suggest what measured properties (features) might be useful for pattern recognition prediction of cell performance in a *supervised* procedure, i.e. predicting

TABLE 5

Statistical differences in means of suspected cell clusters vs. control groups in CEMC capacity test. Mar. 1989 and Apr. 1990. *t*-Test applied at 95% confidence level

Group	Cell subsets	Capacity (%) av. ± s.d.		Significant difference	
		1989	1990	1989	1990
Group G1	O/O grid/paste	93.8 ± 0.9	101.7 ± 1.2	yes	yes
(Circuit 1)	O/N grid/paste	92.5 ± 1.2	99.0 ± 1.9		
Group G2	outer cells	93.6 ± 1.3	101.7 ± 0.7	no	no
(Circuit 2)	inner cells	93.8 ± 2.3	100.9 ± 2.3		
Group G3	O/N grid/paste	93.5 ± 1.6	99.4 ± 1.5	yes	yes
(Circuit 3)	N/N grid/paste	97.8 ± 2.2	102.2 ± 2.3		
Group G4	outer cells	98.8 ± 2.7	104.1 ± 3.1	no	no
(Circuit 4)	inner cells	96.8 ± 2.6	103.0 ± 2.5		
Group G5	observed cluster	90.7 ± 1.5	97.0 ± 1.1	yes	no
(Circuit 1)	control set	92.5 ± 1.2	99.0 ± 1.9		
Group G6	observed cluster	97.2 ± 0.4	103.6 ± 0.7	yes	yes
(Circuit 2)	control set	94.4 ± 1.6	101.9 ± 1.5		
Group G7	observed cluster	87.2 ± 0.6	96.2 ± 0.2	yes	yes
(Circuit 2)	control set	94.6 ± 1.7	102.3 ± 1.2		

Nos. of cells in each subset were: G1(6, 18); G2(5, 6); G3(11, 12) (1989), (11, 18) (1990); G4(15, 10) (1989), (19, 12) (1990); G5(4, 18); G6(5, 26); G7(2, 21) (1989), (2, 15) (1990).
Refer to Table 4 for designated cluster groups.

performance of new cells based on known multivariate distributions of previously observed performance of similarly manufactured cells. This possibility is explored here with the GNB battery data and results are discussed below.

The possibility of using periodic maintenance data for predicting subsequent cell performance is intriguing also because, if successful, this strategy might substitute for periodic cell capacity tests, or provide early indication of imminent cell failures in large battery installations where capacity tests are not practical. Because of the extensive detailed maintenance data base accumulated for the GNB battery over its lifetime, this kind of data analysis was attempted, and the results are discussed here.

Performance prediction from maintenance data

The data base examined so far includes all maintenance data (float voltages, specific gravities, water added, electrolyte levels) collected quarterly between Aug. 1987 and Feb. 1990. Multivariate analysis methods were used to determine if cell capacities, obtained in Mar. 1989 and Apr. 1990, could be predicted from the preceding maintenance data.

The utilization of multivariate analysis techniques was dictated by the fact that no obvious univariate correlations existed between the maintenance data and cell capacities. The techniques used included: correlation analysis, *K*-nearest neighbor pattern recognition and non-linear mapping (see 'Introduction' and refs. 1–6).

The feasibility of pattern recognition performance prediction was tested, first, by creating a training set of maintenance data collected prior to the Mar. 1989 capacity test at CEMC. The maintenance data were organized into a SYMPHONY™ data base containing 38 different descriptors for each cell. These descriptors included: float voltage (CELVOLT), specific gravity (SPGR), water added (WATER) and electrolyte level (LEVEL), collected quarterly between Aug. 1987 and Feb. 1989 (24 total descriptors), as well as 14 computed or combined descriptor values (average values: AVGVLT, AVSPGR, AVWAT, AVLVL), (trends: DVL2/1, DVL7/1, DSG2/1, DSG7/1, DW7/1, DLEV2/1, DLEV7/1), (combined values: ASG*AVL, AVL/ASG, PVLT). Where 'ASG' and 'AVL' refer to AVSPGR and AVGVLT, the average values of specific gravity and cell voltage over the preceding four maintenance events. Trend values ('xxxN/M') refer to differentials between the *N*th and *M*th quarterly maintenance events preceding the capacity test (e.g. for this training set, 'DVL2/1' refers to the change in cell voltage between the next last and last quarterly maintenance measurements, Nov. 1988 and Feb. 1989.) 'PVLT' defines a feature obtained from the product of measured cell voltages over four maintenance quarters preceding the capacity test.

Obviously, many additional computed/combined descriptors might be defined, and future work will consider this. However, this initial set of 38 descriptors was deemed sufficiently representative of maintenance data variance for initial pattern recognition studies.

The first step involved selecting a manageable subset of descriptors (features) for pattern recognition. Arbitrarily the maximum number of features examined at one time was limited to 15. Thus, correlation analysis was conducted first to determine which features were highly correlated, so that redundant features could be eliminated. All features were normalized to the same numerical scale by autoscaling [3, 7]. This step was followed by pattern recognition studies designed to separate maintenance data patterns into one of three classes: high capacity, low capacity, and intermediate capacity cells. Less useful features for this function were likewise eliminated until a minimal useful set of features was obtained.

To determine if maintenance patterns could classify cell performance, the cells were rank ordered according to capacity (measured 3/89). Those cells with capacity values > (av. + 1 s.d.) were assigned to class 1 (high); those cells with capacity < (av. − 1 s.d.) were assigned to class 2 (low); those in between were assigned to class 3 (intermediate). The average value for 109 cell capacities (3/89) was 95.0%; the s.d. was $\pm 3.1\%$. Thus, class 1 cells (17) had capacities $>98.1\%$; class 2 cells (14) had capacities $<91.9\%$; class 3 cells (78) had capacities from 91.9 to 98.1%. For pattern recognition purposes class 3 was reduced to only 14 representative cells in order to have three nearly equal size classes.

A pattern set which included only class 1 and class 2 cells was examined first, in order to identify those features which could readily discriminate between high- and low-capacity cells. Pattern recognition results for the two-class set showed that several different combinations of maintenance features could classify cells into high-or low-capacity classes with 100% accuracy. The various feature sets giving this high accuracy are listed in Table 6.

The results for the three-class pattern set are summarized in Table 7. They showed that overall classification accuracy as high as 83% could be obtained with as few as four features. Not surprisingly, the overall accuracy is not as good as for the two-class set. This is probably because the boundaries between the high/low-capacity classes and the intermediate class are somewhat diffuse. This can be seen in the non-linear mapping displays of the feature spaces used for pattern recognition (Figs. 6(a) and (b)). Figure 6(a) shows a clear-cut discrimination between class 1 and class 2 patterns in feature space, whereas Figure 6(b) shows that the intermediate class 3 patterns tend to extend beyond the boundaries of both class 1 and class 2 patterns.

TABLE 6

Pattern classification training results for two-class pattern set. Maintenance data collected prior to Mar. 1989 capacity test

Overall classification accuracy (%)	Classification accuracy (%)		Features used
	Class 1	Class 2	
100	100	100	PVLT, DVL7/1
100	100	100	CELVOLT(2), SPGR(3)
100	100	100	[PVLT/(DVL7/1)], DSG7/1, DLV2/1, AVGVLT, AVSPGR
100	100	100	CELVOLT(1), ASG*AVL, AVL/ASG, WATER(7), LEVEL(3)

Total patterns = 28.
Class 1 = high capacity cells (14).
Class 2 = low capacity cells (14).

TABLE 7

Pattern classification training results for three-class pattern set. Maintenance data collected prior to Mar. 1989 capacity test

Overall classification accuracy (%)	Classification accuracy (%)			Features used
	Class 1	Class 2	Class 3	
81	92.9	78.6	71.4	DW7/1, CELVOLT(2), CELVOLT(1), ASG*AVL
81	100	71.4	71.4	PVLT, DVL2/1, DW7/1, CELVOLT(3)
83	100	78.6	71.4	DVL2/1, DW7/1, CELVOLT(1), ASG*AVL, WATER(2)
83	85.7	85.7	78.6	CELVOLT(2), WATER(4), WATER(2), AVLVL

Total patterns: 42.
Class 1 = high capacity cells (14).
Class 2 = low capacity cells (14).
Class 3 = intermediate capacity cells (14).

In order to distinguish between fortuitous and meaningful pattern recognition, prediction sets of maintenance data were examined. Here, the maintenance data preceding the Apr. 1990, capacity test were subjected to pattern recognition analysis, using the specific feature sets found useful for classifying the cells from the maintenance data preceding the Mar. 1989 capacity test (see Tables 6 and 7). The important difference for the 'prediction' procedure is that the feature sets represent *new* data, not previously seen by the pattern recognition programs. Thus, the criteria for pattern recognition are based on the feature definitions and combinations useful for the training set data. If these same features are useful also for the prediction set data, and accurately discriminate among the classes of cells, this is a significant observation.

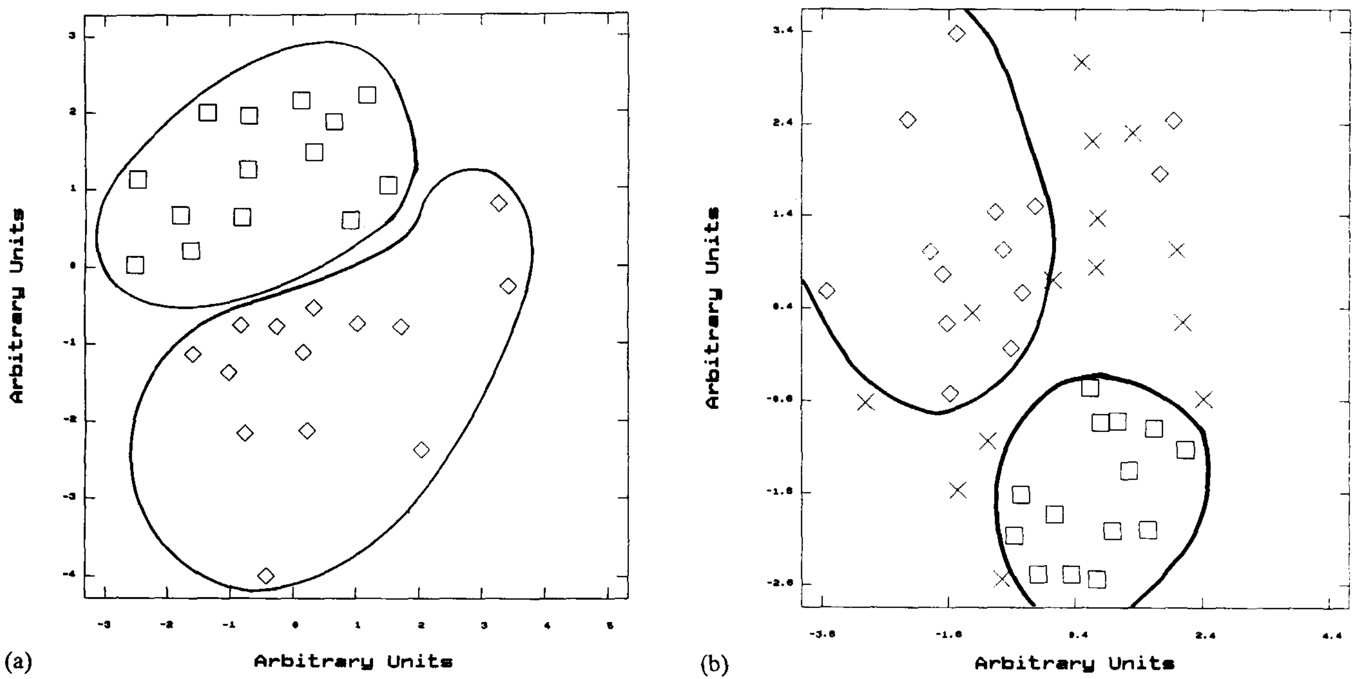

(a) (b)

Fig. 6. Non-linear mapping (NLM) of GNB cell maintenance features. Data collected at CEMC prior to Mar. 1989 capacity test. Features used for pattern recognition capacity classification (see Tables 6 and 7). □ = High-capacity cells (class 1); ◆ = low-capacity cells (class 2); × = intermediate-capacity cells (class 3). (a) Two-class (high/low-capacity classification), successful features: CELVOLT(1), ASG*AVL, AVL/ASG, WATER(7), LEVEL(3). (b) Three-class (high/low/intermediate-capacity classification), successful features; CELVOLT(2), WATER(4), WATER(2), AVLVL.

This would indicate that accurate pattern classification is not fortuitous, and is probably based on a real multivariate relationship between measured maintenance data and observed cell performance.

The Apr. 1990 average capacity (450 A discharge) was 101.5%, ±2.8% standard deviation. Thus, the two-class prediction set contained those cells whose 4/90 capacity was >104.3% (class 1) or <98.7% (class 2). For this preliminary study, only those cells were included in the prediction set which were in the same classes (1 or 2) in both the 1989 and 1990 capacity tests; thus, because of this criterion and differing distributions, there is a slight difference in total numbers of cells analyzed in Tables 6 and 8 (28 versus 23).

When the two-class prediction set based on 4/90 capacity results and the pre-(4/90) maintenance data was examined using the same feature sets identified as useful in Table 6, classification accuracy varied from about 56% to 96%. These results are summarized in Table 8. When a three-class prediction set based on 4/90 capacity results and the pre-(4/90) maintenance data was examined using the same feature sets identified as useful in Table 7, meaningful classification was not obtained.

Observations

It is very encouraging that nearly 100% prediction classification was achieved for the two-class prediction set with one feature set (Table 8). This suggests that performance classification information is indeed contained in the kind of data obtained from quarterly maintenance of flooded lead/acid cells. The inability to accurately predict cell performance divided among three classes is not surprising, considering the fuzzy boundaries illustrated in Fig. 6(b). The most important observation to be made at this point, however, is that cell capacity information sufficient to distinguish between the best and worst performers is most certainly contained in the maintenance data, and that multivariate analysis is effective in extracting that information.

Because the results given here are only preliminary, it is likely that the classification results for the three-class problem will improve considerably with further examination of other possible feature sets and class boundaries. A detailed description of a more

TABLE 8

Pattern classification prediction results for two-class pattern set. Maintenance data collected prior to Apr. 1990 capacity test

Overall classification accuracy (%)	Classification accuracy (%)		Features used
	Class 1	Class 2	
76.2	60	92.3	PVLT, [(DVL7/1)*(DVL2/1)]
55.8	50	61.5	CELVOLT(2), SPGR(3)
96.2	100	92.3	[PVLT/(DVL7/1)], DSG7/1, DLV2/1, AVGVLT, AVSPGR
77.3	70	84.6	CELVOLT(1), ASG*AVL, AVL/ASG, WATER(7), LEVEL(3)

Total patterns: 23.
Class 1 = high capacity cells (10).
Class 2 = low capacity cells (13).

complete study of pattern recognition performance prediction based on routine maintenance data will be presented in a separate publication [14].

Performance prediction from initial fabrication/test data

The purpose of this study was to determine if cell performance at particular stages during its operating lifetime could be predicted from multivariate analysis of initial manufacturer's data. The data base examined is the same as that used for cluster analysis studies discussed here and elsewhere [10, 11], using the descriptive features summarized in Table 1 which led to the kinds of observations summarized in Figs. 1 and 2 and Table 4. The supervised pattern recognition procedure, however, involved the assignment of each cell in a given circuit to a performance class based on known capacity test values.

The cells were rank ordered according to capacity (measured 4/90), with the same class boundaries defined for the maintenance data study. Pattern recognition training results for the two-class pattern set showed that a large number of feature sets could be found from the list in Table 1 which provided as high as 94.9% overall accuracy for identifying cells as class 1 or 2. The most consistently useful features were (refer to Table 1): AVSB, SHPSLFA, EQWC, ASHPA, SG2, EQWF, RELFRMA, AVCAP. As few as 4 or 5 features were required for classification.

Pattern recognition training of a three-class pattern set was conducted, again with the same boundaries as defined earlier for the maintenance data study. The results showed that overall classification accuracy as high as 76% could be obtained with as few as four features. In addition, some feature sets were obtained which would provide high accuracy for classifying class 1 and class 2 cells (high/low), while poorly classifying class 3 cells (intermediate). The value of these latter feature sets is to provide a high probability of identifying the high/low capacity cells, while the most probable 'false positives' would be intermediate capacity cells.

When the feature spaces associated with the best two-class and three-class pattern recognition results described above are displayed using a non-linear mapping algorithm, the feature plots in Fig. 7(a) and (b) are obtained. It is very clear from these displays that the high- and low-capacity cells are well separated in feature space (Fig. 7(a)). However, Fig. 7(b) shows that, although the three different classes of cells are distributed separately in feature space, the clusters do overlap somewhat (leading to poorer classification accuracy).

Observations

The most important observation to be made at this point is that late-life cell capacity information is most certainly contained in manufacturer's initial fabrication/test data, and that multivariate analysis is effective in extracting that information. This conclusion is clearly established in the two-class pattern recognition training results and the feature space plots of Fig. 7.

Because the results given here are only preliminary, it is expected that the classification results for the three-class problem will improve considerably with further examination of other possible feature sets and class boundaries. The results are very encouraging, and more detailed studies and results will be reported elsewhere [15].

Global observations

It is appropriate now to consider some global aspects of the GNB battery study, incorporating observations related to the entire lifetime of the cells to date.

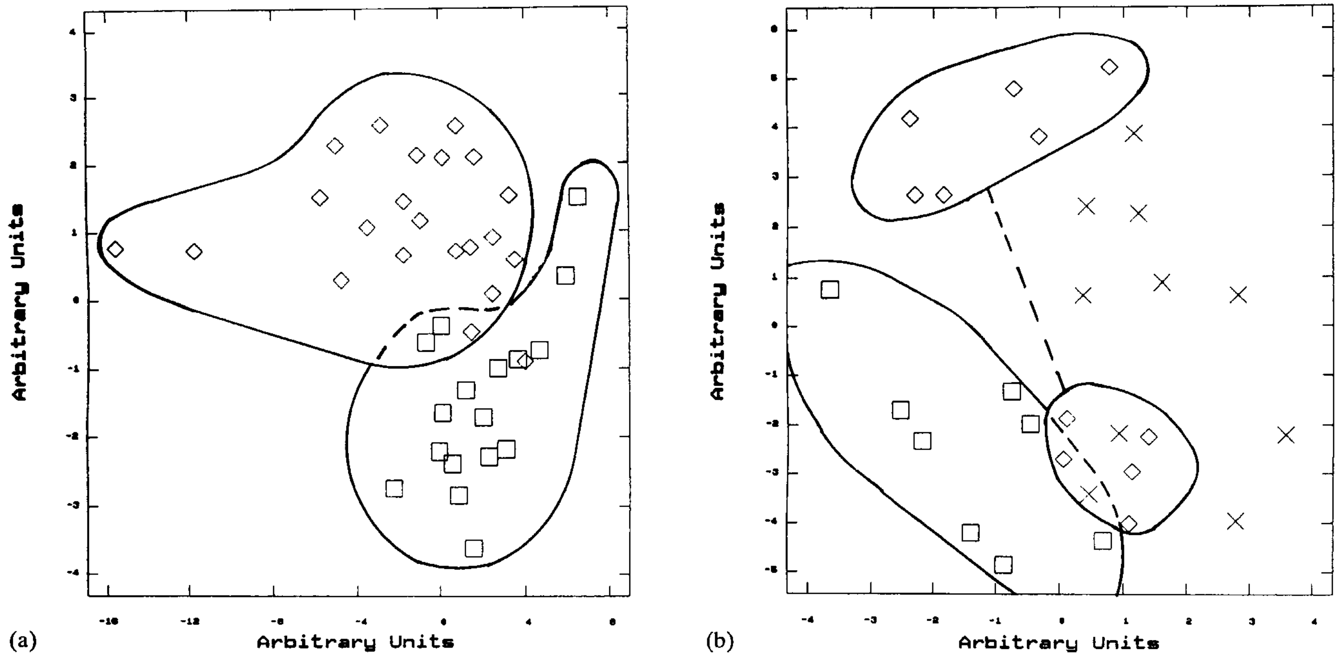

Fig. 7. Non-linear mapping (NLM) of GNB cell fabrication-test features, used for pattern recognition classification of Apr. 1990 capacity data. □ = High-capacity cells (class 1); ◆ = low-capacity cells (class 2); × = intermediate-capacity cells (class 3). (a) Two-class (high/low-capacity classification), successful features: SG2, EQWC, ASHP, SHPSLFA, AVSB, AVCAP. (b) Three-class (high/low/intermediate-capacity classification), successful features: SG2, EQWF, SG4, ASHPA, SHPSLFA.

Capacity trends

Capacity data were obtained for the GNB 500 kW h lead/acid battery over the period 1983 (manufacturer's capacity test), through 1986 (BEST Facility capacity test), to 1989–1990 (CEMC capacity tests). Examination of these data reveal several problems for the definition of meaningful trends. First, the discharge currents used for 1989–1990 tests are different than the 1983–1986 tests (450 A versus 346.6 A). Second, not all cells have undergone capacity tests at CEMC (for economic reasons).

For the trend analysis reported here capacity data for four separate periods of battery lifetime have been included: CAP(I) (initial, all cells) from the 5th and final acceptance cycle, GNB, Sept. 1983 [9]; CAP(II) (early life, end-of-formation, all cells) obtained at the BEST Facility, Jan. 1986); CAP(III) (mid-life, 109 cells) obtained at CEMC, Mar. 1989: CAP(IV) (beginning end-of-life, 121 cells) obtained at CEMC, Apr. 1990.

There are other capacity data which have not been included in these summaries because they are redundant with those above, or because they are unsuitable for trend analysis (different cell groups or very different conditions).

Table 9 summarizes the trends in average cell capacity observed over the four time periods defined above. Only the data for the common subset of 109 cells are included in this Table. The capacities are corrected for initial cell temperatures (NEMA Publication IB 2, 1/17/74) and for variations in discharge current levels (GNB Technical Proposal, Nov. 15, 1982).

It is clear that the variance in average capacity from test to test includes contributions other than temperature and discharge current variance. In order to examine capacity trends for individual cells, the contributions to absolute capacity differences due to variations in test conditions (for example, different usage by CEMC prior to capacity tests) were minimized by obtaining 'normalized capacity values'. These were computed by taking the ratio of the observed cell capacity to the average capacity of all cells obtained on the specific date. It is the normalized values that were used to examine trends.

Trend analysis involved computing a linear regression fit to the time dependence of normalized cell capacities, and obtaining the slopes for each cell. Figure 8(a) shows the overall distribution of cells with different capacity trend slopes (%/year). Figure 8(b) shows the dependence of the capacity trend slopes on cell number. It is clear that a bimodal distribution exists. The average slope for change in normalized capacity is slightly positive (+0.42%/yr.) for cell nos. 2–147; and slightly negative for cell nos. 172–319 (−0.53%/yr.). These observations are consistent with the fact that earlier

TABLE 9

Average capacities (%), for 109-cell subset monitored from 1983 to 1990, GNB 500 kW h battery (adjusted to 77 °F and to 346.6 A)

	Test no.			
	I	II	III	IV
Average capacity (%) (adj.)	99.2	109.4	102.6	109.6
Standard deviation	±3.5	±2.9	±3.1	±2.8

100% capacity=2080 A h. I (9/83); II (1/86); III (3/89); IV (4/90).

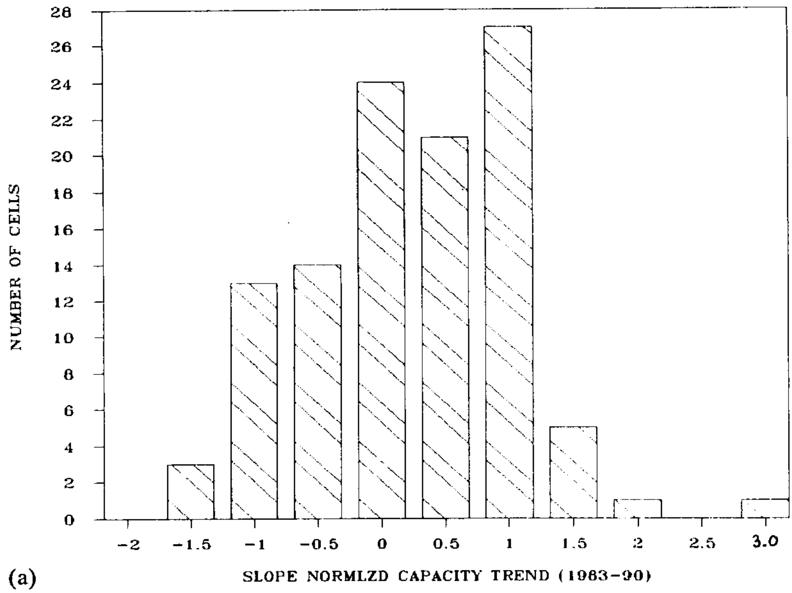

(a)

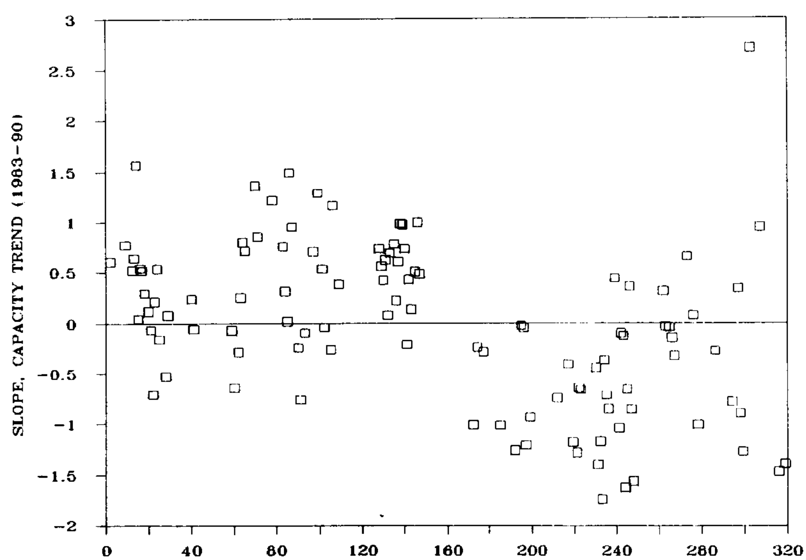

(b)

Fig. 8. Distributions of capacity trend slopes (%/yr.) for GNB cells. Normalized capacities, 109-cell subset monitored, 1983–1990. (a) Overall distribution; (b) distribution by cell number.

numbered cells were less completely formed at the factory in 1983 than the latter cells [9]. Thus, the former cells continued to grow in (normalized) capacity through most of their life to date, whereas the latter group of cells have diminished in (normalized) capacity.

In order to identify those cells which are changing significantly in (normalized) capacity within each of the two subsets identified in Fig. 8, the trend data were examined with respect to the different average trends for the two subsets (subset A, cell nos. 2–147; subset B, cell nos. 172–319). These relationships are illustrated in Fig. 9, which plots the difference between the observed trend slope and the average slope within each of the two regions. Obviously, this transformation leads to a more 'normal' distribution (not bimodal). The list of cells with 'relative' slope for normalized capacity trend steeper than $\pm 0.8\%$/yr. is given in Table 10.

Cell expansion observations

Forty-four of the GNB cells were observed in Oct. 1990 to have expanded noticeably. Five of these exhibited a separation of jar and lid. These observations are summarized in Table 11. None of the cells has failed to deliver adequate capacity, and all have been retained in service until capacity failure is observed.

Some preliminary observations can be made regarding the occurrences of expanded/separated cells.

(i) There is a skewed distribution of swollen cells. The total observed (44) is 13.8% of the 319 cells previously in operation. However, 65.9% of these are for cell numbers above 194.

(ii) Sixteen swollen cells (36.4%) come from formation circuit no. 3 (161–240) and there is a significant disparity in distribution between the two main cell sub-groups from that circuit (see Table 2). The distributions of swollen cells between these two groups are: group (c) (7 swollen cells of 58) 12.1%, and group (d) (9 swollen cells of 22) 40.9%.

(iii) The swollen cells appear in groups of adjacent cells in the same modules. This may be an indication of environmental factors; or that one or more weaker cells in a given module catalyze the degradation of other cells in that module; or of non-uniform conditions established at individual modules (e.g. undetected shipping damage).

(iv) It may be significant that 30% of those cells listed in Table 10 with large negative relative slopes for normalized capacity trend are among the 44 expanded cells.

To determine whether a truly random distribution of swollen cells is occurring, the chi-squared statistical test [13] was applied. The chi-squared test determines whether or not a given frequency distribution is consistent with a normal Gaussian distribution, within some prescribed confidence level. For the CEMC battery observations, the expected frequency of observed swollen cells per module would be 44/54, if the distribution were completely random. That is, an average of 0.81 swollen cells/module should be observed. The chi-squared computation compares the actual distribution to the predicted random distribution. The calculated chi-squared value is 192.2. The tabulated value is 75 at 95% confidence level, 53 degrees of freedom (d.o.f. = no. of modules -1).

Thus, the observed chi-squared value far exceeds the tabulated value, indicating a significant deviation from a predicted random distribution of swollen cells. This observation provides a sound basis for stating that the occurrences of swollen cells are not random; that the above remarks regarding correlations with previously observed fabrication/test data are certainly warranted; and that further consideration is justified of other possible factors (such as undetected shipping damage) affecting this non-random distribution. These observations are very preliminary. There is probably a combination of factors affecting the occurrence of swollen cells. Studies of multivariate

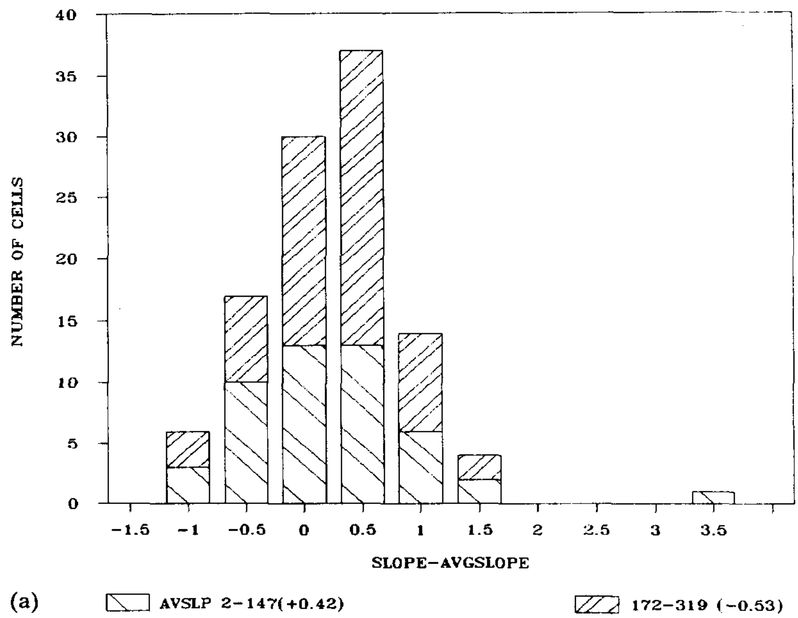

(a)

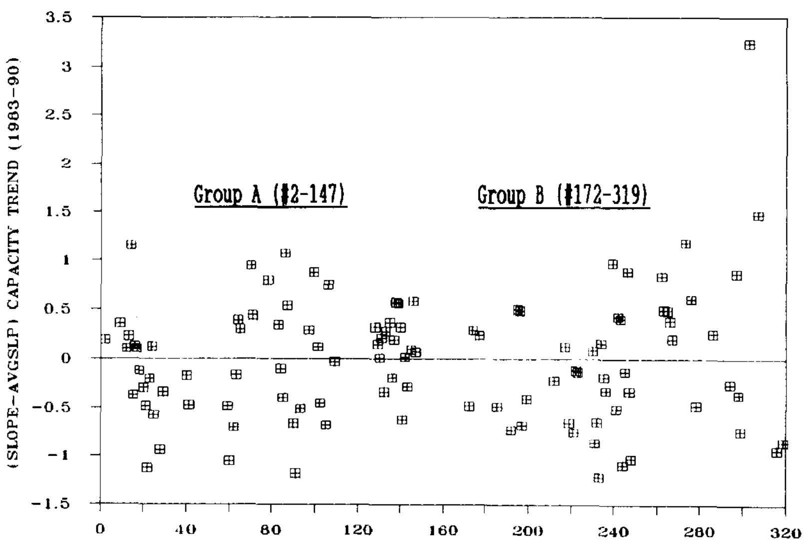

(b)

Fig. 9. Distributions of capacity trend slopes for GNB cells (%/yr.), relative to average slopes in two subsets, cells 2–147 and 172–319. Normalized capacities, 109-cell subset monitored, 1983–1990. (a) Overall distribution, showing contribution of each subset; (b) distribution by cell number, showing each subset.

TABLE 10

Cells identified as having relative normalized capacity trend slopes greater than ±0.8%/yr. Relative slopes compared to average slopes in cell group A (2–147) or cell group B (172–319)

Slope	Cell number
> +0.8%/yr.	14, 70, 86, 99, 239, 246, 262, 273, 297, 303, 307
< −0.8%/yr.	22, 28, 60, 91, 231, 233, 244, 248, 316, 319

TABLE 11

Summary of observed expanded and separated cells; GNB 500 kW h battery, CEMC operation, Oct. 1990

Separated cells		Expanded cells	
Module	Cell no.	Module	Cell no.
2	27, 39	2	26, 27, 30, 37, 38, 39
22	62	22	40, 59, 60, 62, 63
		25	128, 129, 130, 132
		29	195, 197
		30	198, 199, 200, 208, 211
		32	224, 225, 226, 228
		40	205, 206
		42	231, 233, 235
		48	277, 278, 279, 284
49	286, 287	49	285, 286, 287, 291, 294, 295, 296, 297, 299
		50	

correlations with initial fabrication/test data, with periodic capacity test data, and with routine maintenance data might expose the underlying contributing factors.

GNB viewpoint

From a practical standpoint, the observed performance differences are small, and are based on capacity data. These may not be noticed in normal operation, as the battery will seldom experience such a sustained discharge. In any event, capacity values have nearly always been greater than 90%.

Observed 'expansion' of some cells is in the stack-up direction of the cell. Thus, the corrosion of grids over the last seven years has not resulted in grid growth (increase in width or height of the grids) to such an extent as to cause bulging of the jar. It is conceivable that the grid design, with its diamond pattern, accommodates growth much better in the width and height than in the thickness direction. Grid growth in the thickness direction can cause an increase in the stack-up dimension of the plates which might explain the observed 'expansion' of the cell. However, one would expect such growth to occur in all cells and not in just 14–15% of the cells.

An alternate explanation for 'expansion' is that the tray walls are unable to contain the static pressure in the cell. The 54″ span of the side walls of each module were tied together using two keyed partitions located one-third of the way from the end walls. The partitions were made of plywood and coated with resin. With age the keyed locking may have degraded, allowing the walls to bulge at the center. This and the grid growth theory for expansion can be verified and quantified through a tear-down, which will be conducted by GNB, at a suitable time.

Conclusions

The observations made on GNB capacity test data obtained during initial and early-life operation are very striking for several reasons: (i) the cell subsets examined would not have been singled out at all except for the indications from cluster analysis studies done on initial fabrication test data and early-life cycle test data; (ii) the initial cluster analysis studies did not indicate whether future performance of the clusters would be affected, as now observed; and (iii) there is now strong evidence that multivariate cluster analysis studies of initial fabrication test data can predict clustering of cell properties well into their useful lifetime. More importantly, these studies now provide a foundation for interpretation of ultimate cell failure data.

We can only speculate at this time that some of the observed clustering from initial fabrication/test data will correlate ultimately with cell lifetimes, and that the associated features are lifetime predictive. Encouragingly, our earlier work with NiCd [7] and (Exide EV-106) lead/acid [8, 10] cells successfully demonstrated pattern recognition lifetime prediction from initial test data.

The results of preliminary studies of pattern recognition performance prediction from examination of routine maintenance data or initial manufacturer's data are very encouraging. We expect that more detailed studies of these data sets will identify multivariate relationships which may be generally useful for lead/acid cells.

Regarding the benefits of this work, the relationships examined in this study, between process variables and performance variations observed in applications, provide important information to battery companies. Reduction in such performance variations is mutually desirable to both manufacturer and customer, particularly for applications to large battery arrays. Users of very large battery arrays, such as utilities in load/power management applications, can use multivariate analysis studies like ours to gain early identification of problems, trends, and the relationships between performance and site specific conditions as well as manufacturing process variables.

Acknowledgements

The authors are grateful to the Electric Power Research Institute and San Jose State University for support of this work. The authors also thank Al Pivec and Lloyd Weatherman for assistance in planning and directing the capacity tests at CEMC.

References

1 H. C. Andrews, *Introduction to Mathematical Techniques in Pattern Recognition*, Wiley–Interscience, New York, 1972.
2 K. Varmuza, *Pattern Recognition in Chemistry*, Lecture Notes in Chemistry, Vol. 21, Springer, New York, 1980.
3 M. A. Sharaf, D. L. Illman and B. R. Kowalski, *Chemometrics, Chemical Analysis*, Vol. 82, Wiley–Interscience, New York, 1986.

4 D. L. Massart, B. G. M. Vandeginste, S. N. Deming, Y. Michotte and L. Kaufman, *Chemometrics: a Textbook, Data Handling in Science and Technology*, Vol. 2, Elsevier, Amsterdam, 1988.
5 J. W. Sammon, *IEEE Trans. Comput., C-18* (1969) 401.
6 K. Fukunaga, *Introduction to Statistical Pattern Recognition*, Academic Press, New York, 1972, Ch. 10.
7 W. A. Byers and S. P. Perone, *J. Electrochem. Soc., 126* (1979) 720.
8 S. P. Perone and W. C. Spindler, *J. Power Sources, 13* (1984) 23.
9 R. N. McClellan and S. L. Deshpandé, 500 kW h lead-acid battery for peak-shaving, energy storage; testing and evaluation, *EPRI-EM3707*, Oct. 1984.
10 S. P. Perone and W. C. Spindler, in L. J. Pearce (ed.), *Power Sources 10, Proc. 14th Int. Power Sources Symp., Brighton, UK, Sept. 1984.*
11 S. P. Perone and W. C. Spindler, *Proc. 2nd Int. Conf. Batteries for Utility Energy Storage, Newport Beach, CA, July 24–28, 1989*, Special Technical Publication, Electric Power Research Institute, Palo Alto, CA, July 1989.
12 S. P. Perone, W. C. Spindler and S. Deshpandé, *Proc. 3rd Int. Conf. Batteries for Utility Energy Storage, Kobe, Japan, Mar. 18–22, 1991.*
13 J. C. Miller and J. N. Miller, *Statistics for Analytical Chemistry*, Ellis Horwood, Chichester, UK, 1984.
14 S. P. Perone and P.-H. Chen, *J. Power Sources,* to be submitted.
15 S. P. Perone and R. Petesch, in preparation.